The heat source at the Sengan area is thought to be the complex of the heat from many magma reservoirs which have been effused volcanic rocks intermittently including the Tamagawa Welded Tuffs and andesite volcanoes in these 3 Ma.

References

Itaya, T., Nagao, K., Nishido, H. and Ogata, K. (1984) K-Ar determination of Late Pleistocene volcanic rocks. Jour. Geol. Soc. Japan., 90, 899-909.

Kawano, Y. and Aoki, K. (1960) Petrology of Hachimantai and surrounding volcanoes, northeastern Japan. Sci. Rept. Tohoku Univ., Ser III, 6, 409-429.

Mankinen, E.A. and Dalrymple, G.B. (1979) Revised geomagnetic time scale for the interval 0-5 m.y. B.P. Jour. Geophy. Res., 84, B2, 615-626.

Nakamura, H. and Sumi, K. (1981) Takinoue geothermal field, in Yuhara, K., ed., Field Excursion guide to geothermal fields of Tohoku and Kyusyu, Volc. Soc. Japan, 13-21.

Suto, S. (1985) Volcanic activity during Pliocene to Pleistocene in southern part of the Sengan (Hachimantai) geothermal area, northeast Japan - Paleomagnetic study and age determination of andesite volcanoes. Bull. Geol. Surv. Japan, 36, 513-533. (in Japanese with English abstract)

Suto, S. (1978) Large scale felsic pyroclastic flow deposits in the Sengan goehtermal area, northeast Japan - Tamagawa and Old Tamagawa Welded Tuffs -. Rept. Geol. Surv. Japan, 266, 77-142. (in Japanese with English abstract)

Suto, S. and Ishii, T. (1987) Geology of the Shizukuishi district with Geological Sheet Map at 1:50,000. Geol. Surv. Japan, 1-142. (in Japanese with English abstract)

Suto, S. and Mukoyama, S. (1987) Volcanic history at northern part of the Sengan geothermal area, northeast Japan, on the basis of paleomagnetic study. Rept. Geol. Surv. Japan, 266, 143-158. (in Japanese with English abstract)

Takaoka, N., Konda, T., Oba, Y., Konno, K., Iida, M., Sudo, H., Hanzawa, K. and Minamidate, Y. (1988) K-Ar age determination of the volcanic rocks, younger than 1 Ma. Absolute age determination of the volcanic rocks, younger than 1 Ma, 1-43. (in Japanese)

Table 3. K-Ar age data

Loc No.*	No. of Specimen	Rock**	Latitude Longitude	No. in Laboratory	K (wt %)	Rad.argon 40 (10^{-8}cc STP/g)	K-Ar age (Ma)	Air conc. (%)
21	AZ-10	Qz-bg cpx-opx andesite	39°51'41"N	S12-79	0.62	4.07±0.39	1.96±0.17	85.3
			140°51'52"E	S12-101	±0.02	3.97±0.38	1.65±0.17	85.5
							av. 1.67±0.12	
19	1886	Opx-cpx andesite	39°51'27"N	S12-88	0.59	3.31±0.22	1.37±0.10	80.5
			140°53'29"E	S12-113	±0.02	3.20±0.23	1.40±0.11	81.4
							av. 1.39±0.08	
16	MT-4	Opx-cpx andesite	39°51'23"N	S12-85	0.89	4.26±0.71	1.23±0.21	91.4
			140°54'21"E	S12-110	±0.03	4.64±0.71	1.34±0.21	90.5
							av. 1.29±0.15	
24	KI-16	Qz-bg cpx-opx andesite	39°51'50"N	S12-90	0.82	4.89±0.19	1.54±0.08	67.7
			140°51'02"E	S12-111	±0.03	5.09±0.19	1.60±0.08	67.7
							av. 1.57±0.06	
17	MT-3	Cpx-ol-opx andesite	39°50'50"N	S12-86	0.08	0.23±0.18	0.74±0.59	98.1
			140°54'31"E	S12-109	±0.01	0.37±0.18	1.19±0.59	96.9
							av. 1.07±0.50	
18	1885	Ol-cpx-opx andesite	39°50'55"N	S12-89	0.50	0.91±0.14	0.47±0.07	90.8
			140°54'00"E	S12-112	±0.02	0.86±0.15	0.44±0.08	91.7
							av. 0.46±0.05	

The constants for the age calculation are : $\lambda_\beta=4.962\times10^{-10}/y$, $\lambda_\varepsilon=0.581\times10^{-10}/y$, $K^{40}/K=1.167\times10^{-4}$.
*Numbers in Fig. 2. **qz:quartz, cpx:clinopyroxene, opx:orthopyroxene, ol:olivine, bg:bearing

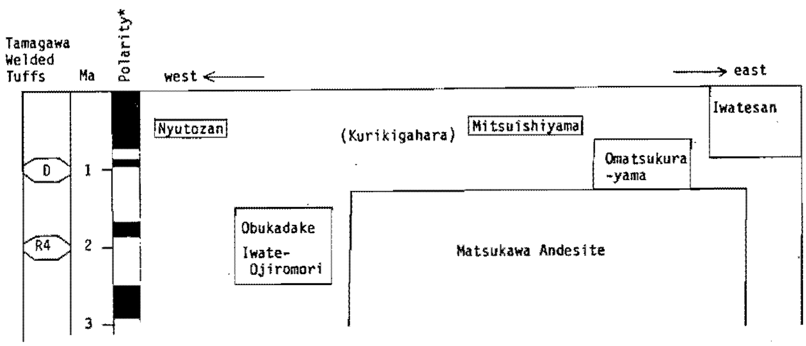

*: Polarity time scale from Mankinen and Dalrymple (1979)

Fig. 5. Volcanic succession of the Matsukawa-Kakkonda area. Age data are quoted from Itaya et al. (1984), Takaoka et al. (1988), Suto (1985, 1987) and this study. Paleomagnetic data are quoted from Suto (1985), Suto and Ishii (1987), Suto and Mukoyama (1987) and this study.

GEOLOGICAL ANALYSIS OF THE KAKKONDA GEOTHERMAL RESERVOIR

DOI, N., MURAMATSU, Y., CHIBA, Y. and TATENO, M., Geothermal Development Division, Japan Metals and Chemicals Co.,Ltd., 24 Ukai, Takizawa-mura, Iwate-gun, Iwate Prefecture 020-01, Japan

INTRODUCTION

Detecting the distribution of permeable fractures in order to develop the geothermal reservoirs successfully is one of the most important part of analysis. And, it is also useful to know the fracture's genesis in order to estimate the distribution of the fracture in the poorly surveyed field. In this paper, fracture distribution and its genesis will be discussed in connection with a geological subsidence, folding, and magma intrusion.

Kakkonda (Takinoue) geothermal field is located in Iwate Prefecture, Japan (Fig. 1), and is a hot water dominated geothermal resevoir. A 50MW geothermal electric power plant was put into operation in 1978 by JMC and Tohoku Electric Power Co., Ltd.. The plant is operated by eighteen production wells of 890-1820m in depth, and all of the separated hot water is injected by sixteen reinjection wells of 520-1600m in depth.

Seven production and seven reinjection wells have been newly drilled for another 50 MW geothermal power plant. These deep wells reveal the geological condition such as fractures, dykes, hornfels and temperature distribution in deeper depth.

OUTLINE OF FRACTURE DISTRIBUTION

There are three types of permeable fractures in the genesis.

Type 1: an intensely fractured zone formed by the subsidence of the field
Type 2: fractures formed by folding
Type 3: fractures formed by magma intrusion

Types 1 and 2 are estimated to be related each other in the genesis.

Fractured rocks are Miocene marin formations, which are divided into the Kunimitoge, Takinoue-onsen and Yamatsuda Formations in ascending order. The lower limit of the Kunimitoge Formation is not yet found in the deepest well of 2126m (-1440m S.L.). These three formations are composed of andesitic lapilli tuff, tuff breccia, dacitic pumice tuff, lapilli tuff, black shale, andesite (Kunimitoge F.), dacitic tuff, lapilli tuff, black shale (Takinoue-onsen F.), dacitic lapilli tuff, sandstone and siltstone (Yamatsuda F.). These fractured rocks are overlain by Plio-Pleistocene Tamagawa Welded Tuffs and Pleistocene andesite lava flows.

VERIFICATION OF THE INTENSELY FRACTURED ZONE FORMED BY THE SUBSIDENCE

Fig. 1, the most permeable zone in the field which is 1000-1600m in depth, shows the intensely fractured zone. This includes the five drilling sites A, B, C, D and E in the electric power plant.

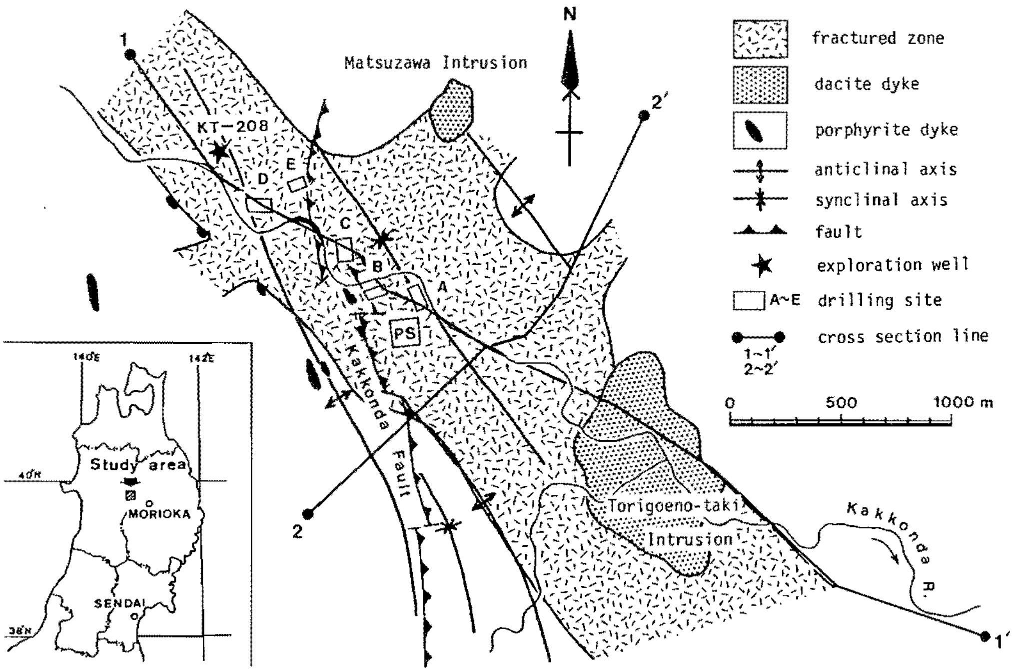

Fig. 1. Schematic map of the geological structure and dyke.

The fractured zone mainly extends in the NW-SE direction, and also extends branches toward the NE-SW direction. This distribution pattern indicates that the fractured zone is an assembly of many fractures in the same direction. Nakamura and Sumi (1981), Sato (1982) and Nakamura et al. (1984) have described faults in the same directions, and EW direction.

The fractured zone is roughly located in the synclinal structure and bounded on both sides by anticlinal axes except for the D drilling site (Figs. 1 and 2). But, the fractured zone extends to the southeast area where a homoclinic structure developed. The formation temperature in the fractured zone has been remarkably changed by the production and reinjection of geothermal fluid during the past ten years.

Sato (1982) shows the distribution map of the Bouguer anomalies in the field, and suggests that the surface geological structure trends in NW-SE and NE-SW directions. The NW-SE low gravity anomaly along the Kakkonda River suggests the subsidence of the area. The geological survey for the exploration well (AZE-1) drilled at the northern part of this low gravity anomaly clarified the thinner thickness (230m) of the Kunimitoge F. compared with the Kakkonda field (1570m+)(Ogasawara et al., 1986). This evidence suggests the subsidence of the Kakkonda geothermal field in the eary to middle Miocene age.

FRACTURES FORMED BY FOLDING

Sato (1982) has described the relationship between fractures and folding. Extension fractures develop in the trough of a syncline, and slip plane (bedding plane) of argillaceous rocks and others with exception of an anticline. Sato has also described that the anticline was formed by the combined mechanisms of bending and flexural flow, and that the syncline was probably formed by buckling associated with flexural slip.

Fig. 3 shows the lithology, circulation loss and temperature log for the KT-208 exploration well. The KT-208 well is nearly vertical and is located on a west limb of an anticline in the fractured zone (Fig. 1). Many circulation losses occurred during drilling. The temperature log indicates some zones of different permeability. There are permeable zones, 0-300m; impermeable zones, 300-1000m; permeable zones, 1000-1400m; comparatively impermeable zones, 1400-2126m (well bottom). At the depth of 1400m to 1500m, the temperature increases abruptly from 266 to 332°C, because the geothermal fluid, with a temperature of about 260°C, flows into the permeable zone (1000-1400m in depth) toward the D production site through this well. At 1400-2126m in

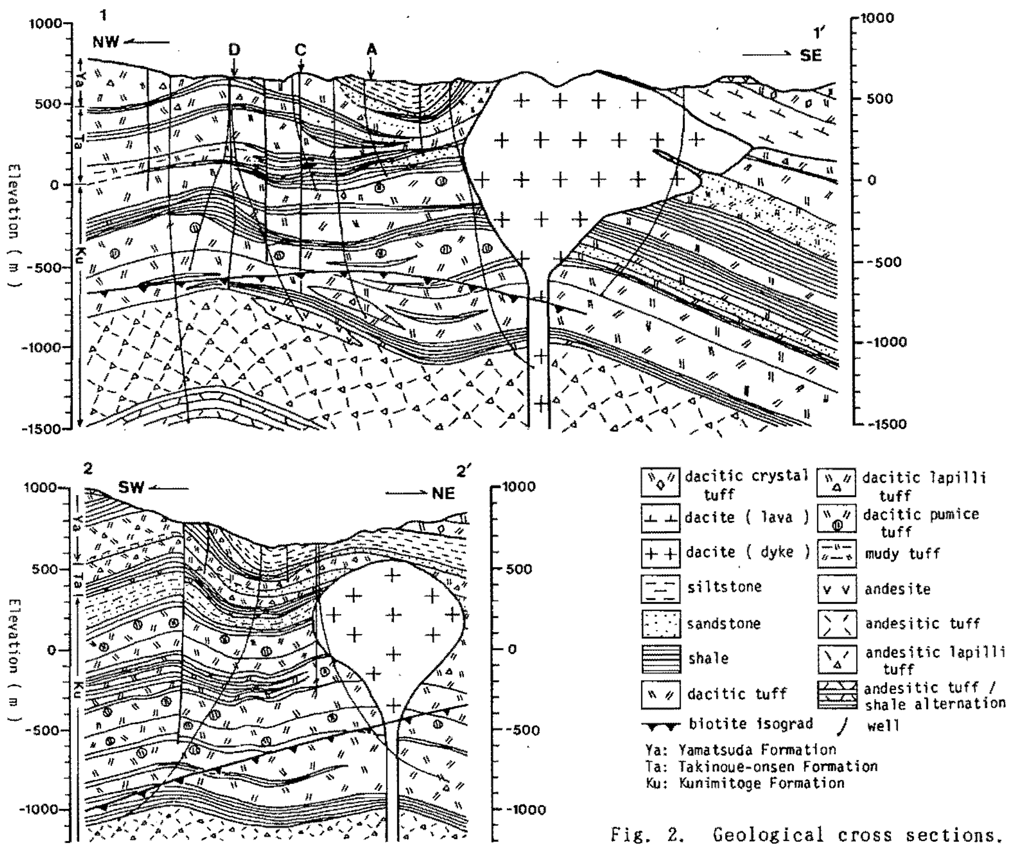

Fig. 2. Geological cross sections.

depth the comparatively impermeable zone remains at an almost constant temperature.

The distribution of the vein and the fracture together with the slickenside has been surveyed using core samples from the KT-208 well which is 690-1290m in depth. The dip meter and bore hole televiewer surveys have also been carried out at 690-1290m and 1020-1150m in depth by Schlumberger Japan Inc. and Geological Survey of Japan, respectively. Fig. 4 shows the dip direction of the minor fractures and veins observed in core samples. The exact direction of the fracture and vein has been obtained by coinciding the orientation of core fracture with dip meter log at 1220-1310m in depth. This figure shows that most of the fractures and veins are in the direction of MN 30° W and 20-50° SW dip, and in the directions of NE-SW and EW. The bedding plane trends MN 30° W (Fig. 1) and dip 25-48° SW. So, about 50% of fractures and veins are almost parallel to the bedding plane, and about 35% of them dip at a higher angle.

In black shale (690-890m in depth), although there are more fractures and veins than in the dacitic tuff (Fig. 5), they do not contribute to the fluid flow so much. The permeable zone in the dacitic tuff is composed of three or more faults with minor fractures and veins around the axial plane and east of it. These permeable fractures (faults) are considered to be formed by the flexural folding.

FRACTURES FORMED BY MAGMA INTRUSION

The dyke rocks in the Kakkonda field are composed of altered dacite and porphyrite (Fig. 1), and fresh pyroxene andesite which forms a minor dyke swarm in the subsurface. Dacite dykes are Matsuzawa and Torigoeno-taki Intrusions. The Matsuzawa Intrusion (magma vol. 0.3 km^3) has the hypabyssal(quartz porphyrite)-plutonic(tonalite) facies, and poor fractures in the intrusion body (Doi et al., 1988). But, the margin of dyke has been fractured and accompanied with white-coloured silicified wall rock (mainly dacitic tuff) zone with 100-200m in width, and is a superior production zone.

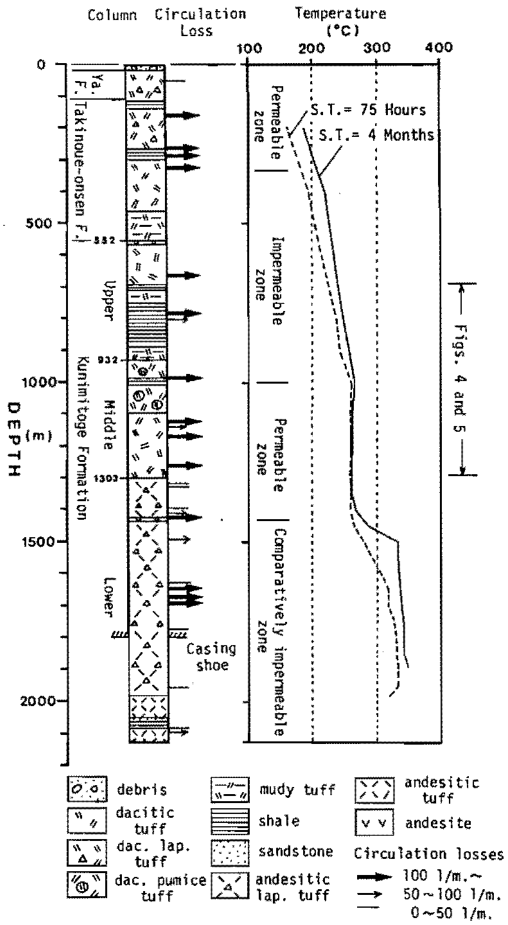

Fig. 3. Lithology, circulation loss and temperature log of the KT-208 exploration well.

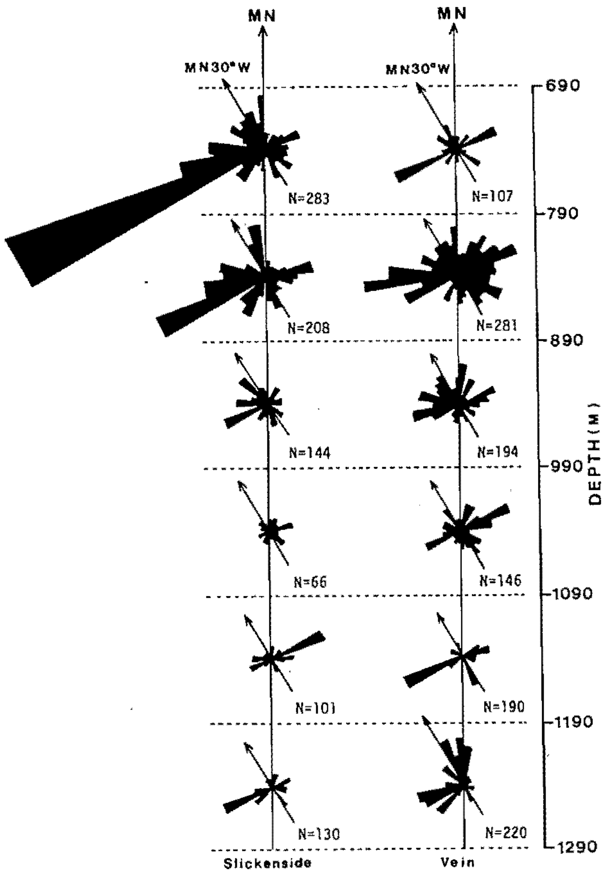

Fig. 4. Distribution of dip direction in the fracture and the vein observed in the core samples of the KT-208 well.

The Torigoeno-taki Intrusion (1.0-1.5 km^3) has a ballon shape (Figs. 2 and 6), and is partly effusive rock (lava dome). The dyke has only volcanic (dacite) facies at the 1800m depth. Wells have crossed with the dyke 57 times, and have met with circulation losses eight times at 700- -500m S.L.. Circulation losses have occurred 17 times in the intrusion at 300- -300m S.L., too. In these depth, the dyke expands laterally, especially toward SE direction where it intercalates dacitic lapilli tuff with molluscan shells (Yamatsuda F.) in it (Fig. 2). Circulation losses at the margin and in the dyke suggests magma fracturing to the wall rock and flexural flow in the viscous dacite magma.

CONCLUSION

There are three types of fractures in the Kakkonda geothermal field. One is a intensely fractured zone formed by a subsidence. Second is a fracture formed by a flexural folding. And last is a fracture formed by magma fracturing and a flexural flow in a viscous magma.

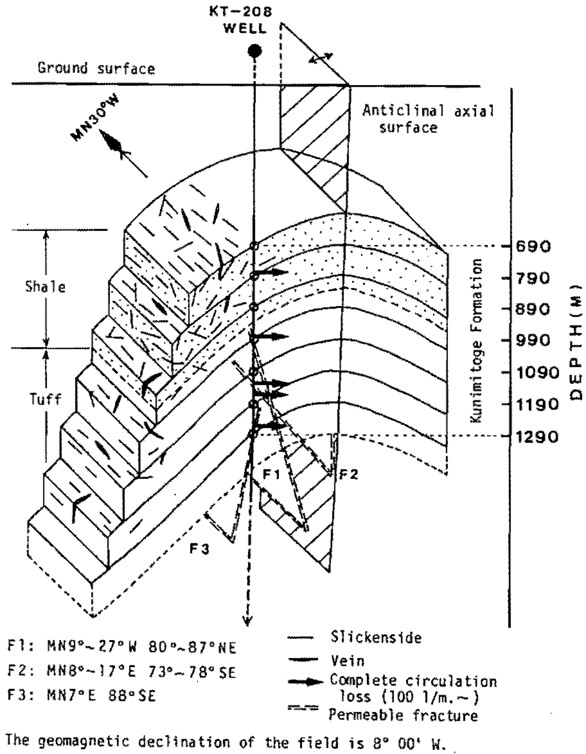

Fig. 5. Schematic relation between anticlinal structure and fracture in the KT-208 well.

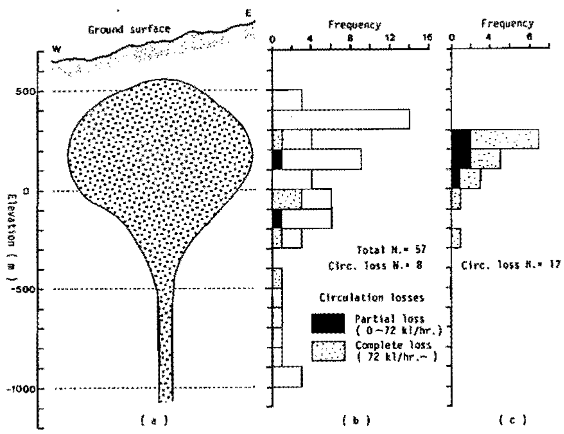

Fig. 6. Fracture at the margin and in the Torigoeno-taki Dacite Intrusion. (a) shape of the Torigoeno-taki Dacite Intrusion, (b) frequency of intersection with the dyke and circulation loss at the margin, (c) frequency of circulation loss in the dyke.

REFERENCES

Doi, N., Kudo, H., Takanohashi, M. and Niitsuma, H. (1988) AE measurement and fracture behavior during hydraulic fracturing in the Kakkonda geothermal field, Japan. Jour. Geother. Res. Soc. Japan, 10, 3, 237-249*.

Nakamura, H. and Sumi, K. (1981) Exploration and development at Takinoue, Japan. Geothermal System: Principles and Case Histories, Edit. Rybach, L. and Muffler, L. J. P., John Wiley & Sons Ltd., 247-272.

Nakamura, H., Sato, K., Chiba, Y. and Miyazaki, S. (1984) Characteristics of fracture in the Kakkonda (Takinoue) geothermal area, Iwate Prefecture. Jour. Japan Geother. Energy Associ., 21, 271-281*.

Ogasawara, K., Maruyama, T., Doi, N., Yoshida, T. and Matoba, Y. (1986) Island arc transverse route, No. 16. Geol. Data Northeast Honshu Arc in Neogene Era, Edit. Kitamura, N., 2, 4, 1-13**.

Sato, K. (1982) Analysis of geological structure in the Takinoue geothermal area. Jour. Geother. Res. Soc. Japan, 3, 135-148.

* in Japanese with English abstract.
** in Japanese.